HHS Public Access

Author manuscript

Lab Invest. Author manuscript; available in PMC 2011 February 01.

Published in final edited form as:

Lab Invest. 2010 August ; 90(8): 1152–1168. doi:10.1038/labinvest.2010.91.

Enterohemorrhagic *E. coli* alters murine intestinal epithelial tight junction protein expression and barrier function in Shiga toxin independent manner

Jennifer Lising Roxas[1], **Athanasia Koutsouris**[1], **Amy Bellmeyer**[1], **Samuel Tesfay**[1], **Sandhya Royan**[1], **Kanakeshwari Falzari**[1], **Antoneicka Harris**[1], **Hao Cheng**[1], **Ki-Jong Rhee**[1], and **Gail Hecht**[1,2]

[1] Department of Medicine, Section of Digestive Diseases and Nutrition, University of Illinois at Chicago, Chicago, IL, USA

[2] Department of Medicine, Section of Digestive Diseases and Nutrition, University of Illinois at Chicago, Chicago, IL, USA; Jesse Brown VA Medical Center, Chicago, IL, USA

Abstract

Shiga toxin (Stx) is implicated in the development of hemorrhagic colitis and hemolytic-uremic syndrome, but early symptoms of enterohemorrhagic *Escherichia coli* (EHEC) infection such as non-bloody diarrhea may be Stx-independent. In this study, we defined the effects of EHEC, in the absence of Stx, on the intestinal epithelium using a murine model. EHEC colonization of intestines from two groups of antibiotic-free and streptomycin-treated C57Bl/6J mice were characterized and compared. EHEC colonized the cecum and colon more efficiently than the ileum in both groups; however, greater amounts of tissue-associated EHEC were detected in streptomycin-pretreated mice. Imaging of intestinal tissues of mice infected with bioluminescent EHEC further confirmed tight association of the bacteria to the cecum and colon. Greater numbers of EHEC were also cultured from stool of streptomycin-pretreated mice, as compared to those that received no antibiotic. Transmission electron microscopy demonstrated that EHEC infection leads to microvillous effacement of mouse colonocytes. Hematoxylin and eosin staining of colonic tissues of infected mice revealed a slight increase in the number of lamina propria polymorphonuclear leukocytes. Transmucosal electrical resistance, a measure of epithelial barrier function, was reduced in colonic tissues of infected animals. Increased mucosal permeability to 4KDa FITC-Dextran was also observed in colonic tissues of infected mice. Immunofluorescence microscopy revealed that EHEC infection resulted in redistribution of the tight junction proteins occludin and claudin-3 and increased expression of claudin-2 while ZO-1 localization remained unaltered. Quantitative real-time PCR revealed that EHEC altered mRNA transcription of Ocln, Cldn2 and Cldn3. Most notably, claudin-2 expression was significantly increased and correlated with increased intestinal permeability. Our data indicate that C57Bl/6J mice serve as an *in vivo* model to study the physiological effects of EHEC infection on the intestinal epithelium and

Corresponding author: Gail Hecht, Department of Medicine (MC716), Section of Digestive Diseases and Nutrition, University of Illinois at Chicago, Room 738A, Clinical Sciences Building, 840 S. Wood Street, (MC 716), Chicago, IL 60612-7323, Phone: 312-996-1565, FAX: 312-996-5103, gahecht@uic.edu.

suggest that altered transcription of tight junction proteins plays a role in the increase in intestinal permeability.

Keywords

C57Bl/6J mice; claudin-2; claudin-3; EHEC; occludin; microvilli effacement; transmucosal electrical resistance

Enterohemorrhagic *Escherichia coli* (EHEC) belongs to a family of pathogenic bacteria that produce attaching and effacing (A/E) lesions used to colonize host intestinal mucosa [1]. Attachment of EHEC to the apical epithelial surface leads to recruitment of cytoskeletal proteins and injection of effector molecules directly into the host cell through the type III secretion system. The A/E phenotype results from expression of virulence genes housed in the locus of enterocyte effacement pathogenicity island that encode proteins for the type III secretion system, intimin, and secreted effector proteins [2].

Shiga-toxin (Stx) is one of the major virulence factors produced by EHEC, and can cause microvascular endothelial injury. Stxs are released by EHEC in the intestine, translocated across the gut epithelium into the circulation, and transported to microvascular endothelial cells. They presumably damage host cells by inhibiting protein synthesis, stimulating pro-thrombotic messages, or inducing apoptosis [3]. Stx has been identified as a critical requirement for the development of hemorrhagic colitis and hemolytic-uremic syndrome, but we hypothesize that in addition, EHEC organisms, in the absence of Stx, have direct effects on the intestinal epithelium that contribute to diarrhea. Early diarrhea caused by EHEC is non-bloody, and is not likely due to Stx. EHEC infection of cultured intestinal epithelial cells induces A/E lesions, alters intestinal epithelial barrier function, modulates ion transport and stimulates inflammation, suggesting that the mechanisms underlying diarrhea associated with infection by this pathogen are complex and multi-factorial [4–6].

Although several experimental animal models have been developed to elucidate EHEC pathogenesis [7–14], the lack of a simple, small murine model has posed a great challenge in understanding EHEC-induced physiological and pathological changes. Moreover, many of the *in vivo* studies focused on the effect of toxin-producing strains. Nagano *et al.* have demonstrated that intragastric inoculation of a Stx-producing EHEC 0157:H7 strain leads to EHEC adherence to intestinal epithelial cells of ICR mice resulting in epithelial cell actin accumulation (characteristic of A/E lesions) [15]. The same group has also reported that fecal shedding of EHEC organisms was observed in ICR mice up to 3 weeks, and the cecum was a frequent site of adhesion and colonization for these pathogenic bacteria. In addition to ICR mice, C57Bl/6J strains have also been used to study the effects of EHEC infection on ion transport [6]. While colonization of EHEC in mice has been demonstrated previously, EHEC-induced pathologic changes have not been fully assessed in mouse models.

Therefore, our goal in this study was to define the effects of EHEC, in the absence of Stx, on the intestinal epithelium using a murine model. We chose to use a Stx-negative derivative of EHEC in order to assess the contribution of virulence factors other than Stx.

Materials and Methods

Bacterial Strains

EHEC O157:H7 strain 85–170, an isogenic Stx-negative derivative [16], (generous gift from James Kaper, Center for Vaccine Development, University of Maryland, Baltimore, MD) was used to infect mice in this study. For permeability experiments, a control group of mice was also orally gavaged with a nonpathogenic human fecal isolate HS-4 [17]. For bioluminescence imaging experiments, EHEC O157:H7 strain 85–170 was transformed with pCM17 plasmid (generous gift from James Kaper, University of Maryland in Baltimore) containing the *lux*CDABE operon driven by the OmpC promoter, which allows constitutive expression of luciferase [18]. Bacteria were grown overnight at 37°C in Luria-Bertani broth, then diluted in serum- and antibiotic-free medium (1:1 (vol/vol) mixture of Dulbecco's modified Eagle's medium and Ham's F12 medium containing 25 mM glucose, 15 mM HEPES and 0.5% (wt/vol) mannose) and grown at 37°C to mid-log growth phase (OD_{600nm}= 0.4).

Infection

Six-week old C57Bl/6J male mice were obtained from Jackson Laboratory (Maine, USA). All animal procedures were approved by the University of Illinois at Chicago Animal Care and Use Committee. Mice were allowed to equilibrate in the Biological Resources Laboratory animal housing facility at the University of Illinois at Chicago for approximately 7 days. Two groups of mice were used in this study: antibiotic-free mice and streptomycin-pretreated mice. The antibiotic-free mice were directly gavaged with EHEC after the 7-day equilibration period. The second group of mice was given water containing 5 g/L streptomycin for 24 hours on the fifth day of their arrival in the facility. The water supply was then replaced with sterile distilled water for another 24 hours prior to infection. Both groups of mice were gavaged with 200 μl of sterile PBS (control, uninfected) or 2×10^8 Stx-negative EHEC organisms suspended in 200 μl sterile PBS.

Attachment Assays

To determine the number of EHEC organisms adherent to the intestinal epithelium, at least four EHEC-infected and uninfected C57Bl/6J mice were sacrificed at days 1, 3, 5, 8, and 10 post-infection. The ileum, cecum, and colon were dissected. Stool contents were removed and tissues were washed with PBS. Tissues were weighed and homogenized in PBS using a Dounce tissue grinder. Homogenized tissues were serially diluted in PBS and plated on MacConkey-Sorbitol agar (BD Biosciences, New Jersey, USA) supplemented with 50 μg/L cefixime and 2.5 mg/L potassium tellurite (Sigma-Aldrich, Missouri, USA), which is a selective and differential media for the detection of sorbitol-nonfermenting *Escherichia coli* 0157:H7. After 18–24 hours of incubation at 37°C, white colonies were counted and colony-forming units (CFU) were determined per gram of tissue. White colonies were confirmed as EHEC by PCR using *espF*-specific primers.

Fecal Shedding of EHEC

Stool samples from at least four uninfected and infected mice were collected daily for a period of 10 days post-infection. Stool samples were weighed and homogenized in PBS by vortexing. Homogenized stool samples were serially diluted and plated on MacConkey-Sorbitol agar supplemented with 50 mg/L cefixime and 2.5 mg/L potassium tellurite. After 18–24 hours of incubation at 37°C, white colonies were counted and CFU were determined per gram of stool.

Bioluminescent EHEC infection and imaging

The protocol for imaging of bioluminescent EHEC was adapted from a previously described *in vivo* bioluminescence imaging of *Citrobacter rodentium* in infected mice [19]. Bioluminescent EHEC was cultured overnight as described above and orally gavaged into streptomycin pre-treated C57Bl/6J mice. Three days after infection, mice were euthanized and entire intestines were excised. The rectum and stomach were tied off and and air injected into the lumen of the intestine to activate the bioluminescence signal. Bioluminescence was determined by IVIS system (Xenogen Corporation, Hopkinton, MA) and expressed as (photons s^{-1} cm^{-2} sr^{-1}). To detect adherent EHEC, cecum and colon tissues were washed extensively with PBS prior to imaging with IVIS.

Transmission Electron Microscopy

The distal small intestine and the proximal colonic tissues were retrieved from uninfected and EHEC- infected C57Bl/6J mice and cut into ~2–3 mm-long pieces and fixed in 4% glutaraldehyde with cacodylate 0.1M buffer. Further routine processing for transmission electron microscopy (TEM) was performed in the Electron Microscopy Facility at the University of Illinois at Chicago.

Histological Staining

Proximal colonic tissues retrieved from uninfected and EHEC-infected C57Bl/6J mice were cut into ~2–3 mm-long pieces and fixed in 10% neutral buffered formalin. Further routine processing for hematoxylin and eosin staining was performed in the Research Resource Center at the University of Illinois at Chicago.

Electrophysiology

At days 1, 3, 5, 8, and 10 post-infection, mice were sacrificed via CO_2 asphyxiation and intestinal tissues were resected. Tissue sections of the proximal colon were mounted in an Üssing chamber for measurement of transmucosal electrical resistance (TER), a previously described indicator of barrier function [20]. Full thickness, unstripped mucosa was bathed on both mucosal and serosal surfaces with 5 ml of oxygenated (95% O_2/CO_2) Ringer's solution containing 109.8 mM NaCl, 5.3 mM KCl, 1.2 mM $CaCl_2$, 1.2 mM $MgCl_2$, 25 mM $NaHCO_3$, 2.4 mM Na_2HPO_4, and 0.4 mM NaH_2PO_4. To maintain tissue viability, 5 mM glucose was added on the mucosal side of the tissue and 5 mM mannitol was added on the serosal side of the tissue.

Permeability Measurements

At day 8 post-infection, mice were sacrificed via CO_2 asphyxiation and intestinal tissues were resected. Upon equilibration of the tissue and measurement of electrical parameters, 4-kD FITC-dextran was added to the mucosal side to achieve a final concentration of 0.01 mM. Permeability (flux) was determined after removal of medium from serosal compartment at the end of a 90 minute experimental period. The medium was then assessed for flourescence using a microplate fluorescence reader (FL-500, BIO-TEK, Vermont, USA) at an excitation wavelength of 485 nm and an emission wavelength of 530 nm.

Immunofluorescence Microscopy

Tissue samples of the proximal colon from all mice sacrificed for Üssing chamber analysis were snap-frozen in optimal cutting temperature embedding medium (Tissue-Tek O.C.T. compound, Sakura Finetek USA, Inc., California, USA) and stored at −80°C. For immunostaining, 5 μm frozen sections were fixed with 1% paraformaldehyde in PBS for 10 min at room temperature. After washing with PBS, permeabilization with 0.5% NP-40, and blocking of nonspecific binding sites with 5% normal goat serum (NGS), tissues were incubated with monoclonal mouse anti-occludin, rabbit anti-ZO-1, rabbit anti-claudin-2, or rabbit anti-claudin-3 (at 0.5 μg/mL, Invitrogen, California, USA) in PBS with 1% NGS for 90 min at room temperature. After washing, sections were incubated with 8 μg/mL Alexa 594-conjugated goat anti-mouse IgG or 8 μg/mL goat anti-rabbit IgG antisera, 5 U/mL Alexa 488-conjugated phalloidin, and Hoechst 33342 (Invitrogen) for 60 min. Sections were then washed and mounted under coverslips using ProLong Gold antifade reagent (Invitrogen). Sections were imaged using a Leica Dm4000B epifluorescence microscope and Slide Book 4.2 software (Intelligent Imaging Innovations, Colorado, USA).

Quantitative Real-time PCR

Four colonic samples for each group of uninfected and infected mice at days 1, 3, 5, 8 and 10 post-infection were analyzed for quantitative real-time PCR (qRT-PCR) using mRNA-specific primers for Ocln, Cldn2, Cldn3 and Gapdh. Tissue samples previously preserved in OCT and stored at −80 °C were microdissected. Nine sections of 10-micron thickness were collected per sample and total RNA was extracted using RNeasy microkit (Quiagen, California, USA). Total mRNA was prepared using First Strand cDNA Synthesis Kit (Fermentas Inc., Maryland, USA). cDNA targets were cloned in pCR®4-TOPO® vector (Invitrogen). Known amounts of serially diluted recombinant plasmids were prepared and served as standards for qRT-PCR. Test samples and plasmid standards were used as templates for qRT-PCR using mRNA-specific primers for Ocln, Cldn2, Cldn3 and Gapdh and Fast Sybr® Green PCR Master Mix (Applied Biosystems, Texas, USA). qRT-PCR reactions were carried out at 50°C for 2 minutes, 95°C for 10 minutes, followed by 40 cycles of 95°C for 15 seconds and 60°C for 1 minute, and a dissociation step at 95°C for 15 seconds, 60°C for 15 seconds and 95°C for 15 seconds using an ABI 7900HT Sequence Detection System (Applied Biosystems). Sequences of primers used are: Ocln forward (5′-agaggctatgggacagggctctttgg-3′), Ocln reverse (5′-ccaacaggaagcctttggctgctcttgg-3′), Cldn2 forward (5′-cctcgctggcttgtattatctctg-3′), Cldn2 reverse (5′-gagtagaagtcccgaaggatg-3′), Cldn3 forward (5′-ccggttcaagtccagcagccatgtc-3′), Cldn3 reverse (5′-gctctgcaccacgcagttcatcc-3′),

Gapdh forward (5′-gaagggctcatgaccacagt-3′) and Gapdh reverse (5′-ggatgcagggatgatgttct-3′). Absolute mRNA copies of the targets were determined per absolute mRNA copies of Gapdh for each sample.

Statistical Analysis

All data are reported as the mean and standard error of the mean. Data comparisons were made with Student's *t* test. Differences were considered significant when the *P* value was ≤0.05.

Results

E. coli O157:H7 colonization of mouse intestines

We tested the ability of *E. coli* O157:H7 to colonize and adhere to the intestines of C57Bl/6J mice after oral gavage of 2×10^8 bacteria with or without streptomycin pre-treatment. EHEC infection of antibiotic-free mice resulted in the colonization of the ileum, cecum and colon (Figure 1A, B, & C). There was a significant (2.2 to 3 log) growth expansion of EHEC attached to ileum, cecum and colon observed at 5 days post-infection in the absence of antibiotics. By 10 days post-infection, EHEC was no longer detected in the intestinal tissue samples of antibiotic-free mice. Greater amounts of tissue-associated EHEC were observed at days 1 and 3 in mice treated with streptomycin prior to infection. In the streptomycin pre-treated mice, growth expansion of EHEC associated with the ileum, cecum and colon also occurred but at 8 days post-infection. In contrast to the antibiotic-free mouse model of infection, EHEC remained detectable (>2 logs/gm of tissue) in the tissue samples even at 10 days post-infection. In both models, EHEC colonizes the cecum and colon more efficiently than the ileum.

Bioluminescence imaging of EHEC in intestinal tissues of infected mice was used to confirm that the bacteria localize and adhere to the cecum and colon (Figure 2). While bioluminescence imaging technique offers easier localization of bacteria in host tissues, it is not as sensitive as culturing tissues or stool from infected animals. Bioluminescence was not able to detect EHEC in tissue sections, such as the ileum, where lower amounts ($< 10^5$cfu/gram of tissue) of colonizing bacteria are found. In order to determine if EHEC intimately adhered to the intestinal epithelium, the intestine from infected animals was opened and washed multiple times in a vigorous fashion in order to remove non-adherent organisms and reimaged. Significant bioluminescent signal was still detected primarily in the cecum and proximal colon, indicating that EHEC tightly adheres to the intestinal epithelium (Figure 2B).

The amount of EHEC shed in the feces was also monitored daily for 10 days. Consistently greater numbers of EHEC were cultured from the feces of mice pre-treated with streptomycin, as compared to those that received no antibiotics (Figure 3). We also observed small (0.5 to 1.5 log), but significant, growth expansion of EHEC in the stool at 8 days post-infection in both infection models. Despite the fact that EHEC was not recovered from intestinal tissues at day 10 in mice that had not received antibiotics, $>10^3$ organisms were cultured per gram of stool.

Alteration of intestinal microvilli following *E. coli* O157:H7 infection

To evaluate the effect of EHEC infection on mouse intestinal epithelial cells, TEM was performed on small and large intestinal segments obtained from uninfected and infected antibiotic-free mice at 1 and 5 days post-infection (Figure 4A & B). While the small intestine and colon of uninfected mice displayed normal microvillous architecture, localized effacement of the microvilli was detected in EHEC-infected mice predominantly in the colon at both 1 and 5 days post-infection. Effacement appeared more extensive and remarkable at 1 day post-infection. Microvillous architecture of the ileum of EHEC infected mice appeared well preserved. Although effacement was evident in the colon, intimately attached bacteria and the well-characterized A/E lesions with pedestals were not readily found by TEM. However, the distortion and effacement of microvilli observed in the colon of EHEC infected mice is consistent with changes induced by enteropathogenic *E. coli* [20]. We also analyzed via TEM the effect of EHEC on the colonic epithelial cells of mice pre-treated with streptomycin (Figure 5). Distortion and localized effacement of the microvilli in the colon was easily identified at 3, 5, 8 and 10 days post-infection. In the colon of infected mice pre-treated with streptomycin, microvillous effacement was most extensive at 3 days post-infection, but was still detectable at day 10 post-infection.

Mild colonic inflammation of mice infected with EHEC O157:H7

To further assess histological changes due to EHEC infection, colonic segments from uninfected and infected mice pre-treated with streptomycin were stained with hematoxylin and eosin. Modest increase in the number of polymorphonuclear leukocytes was found at the lamina propria of mouse colonic tissues at day 3 post-infection as compared to uninfected control (Figure 6), but not at days 1, 5, 8, and 10 post-infection (data not shown).

Disruption of intestinal barrier function in mice infected with EHEC O157:H7

To evaluate the effect of EHEC infection on intestinal epithelial cell barrier function, colonic segments from uninfected and infected mice were mounted in Üssing chambers and electrophysiological parameters were measured. In the antibiotic-free mouse model of EHEC infection, electrical resistance of the colon of infected mice was reduced significantly at days 3 and 5 post-infection when compared to values obtained from tissues of uninfected control mice, suggesting disruption of tight junctions (Figure 7A). In the colon of infected mice pre-treated with streptomycin, resistance values decreased progressively over time, with the maximum reduction detected at 8 days post-infection (Figure 7B). Disruption of intestinal epithelial barrier function was also evaluated by measuring flux of 4-KDa FITC-dextran across colonic segments. Colonic samples were obtained from streptomycin-pretreated mice at day 8 post-infection, where maximum TER reduction was previously observed. A significant increase in mucosal permeability of colonic samples to 4-KDa FITC-Dextran was detected in the colon of EHEC-infected mice (Figure 8A). Colonic samples from a control group of mice orally gavaged with a nonpathogenic human fecal isolate HS-4 had permeability and TER measurements similar to values from uninfected control mice (Figure 8A & 8B).

EHEC infection modifies occludin, claudin-2 and claudin-3 localization in the colon, but not ZO-1

To determine if the physiological changes in the tight junction barrier were accompanied by alterations in the distribution of tight junction proteins, colonic tissues of EHEC-infected and uninfected mice were analyzed using immunofluorescence staining of ZO-1, occludin, claudin-2, and claudin-3. At 1 day post-infection, neither the ileum nor the colon of infected mice showed redistribution of tight junction proteins (data not shown) correlating with the normal electrical resistance measurements. No difference in the distribution or intensity of staining of the intracellular scaffolding protein ZO-1 was seen in the colons of uninfected mice compared to those infected with EHEC (Figure 9) over the course of infection. The transmembrane tight junction protein occludin was also examined in colonic tissues from EHEC-infected and uninfected mice. Occludin was redistributed, specifically internalized, in colonic epithelial cells from animals infected with EHEC (Figure 10), similar to changes reported in mice infected with enteropathogenic *E. coli* [21]. Immunofluorescent staining for claudin-3 revealed staining primarily localized to the lateral membranes, but some intracellular localization was also observed. At 3 days post-infection, claudin-3 staining was clearly diminished (Figure 11). The most interesting results regarded changes in claudin-2. At 1 day post-infection, a slight increase in the amount of claudin-2 within the cytoplasm was noted. However, a more significant and progressive increase in claudin-2 expression, both at the tight junctions and within the cytoplasm, was seen at days 3, 5, 8, and 10 post-infection (Figure 12).

EHEC regulates mRNA transcription of Ocln, Cldn2, and Cldn3

To determine if EHEC-induced perturbation of intestinal epithelial barrier function was associated with altered transcription of genes encoding tight junction proteins, we performed qRT-PCR on colonic samples using specific primers for Ocln, Cldn2, Cldn3 and Gapdh. Total RNA was extracted from microdissected colonic samples of uninfected control and EHEC-infected mice pre-treated with streptomycin. cDNA was synthesized from the total RNA extract, and the product served as template for qRT-PCR. Absolute mRNA copies of Ocln, Cldn2, and Cldn3 per mRNA copies of Gapdh were determined for each sample (Figure 13). Ocln transcription was altered by EHEC infection with a 1- to 1.4-fold decrease occurring at days 3, 5, and 8 post-infection. By 10 days post-infection, there was a significant 1.5-fold increase in the Ocln mRNA transcript levels in the colon of EHEC-infected mice, as compared to uninfected control. EHEC also altered the transcription of Cldn3. At 1 day post-infection, a significant 2-fold increase in transcription occurred. However, thereafter, a progressive decrease in Cldn3 transcription, reaching its lowest level of a 2-fold decrease at 8 days post-infection, was seen. By day 10, Cldn3 mRNA transcripts increased to levels similar to that of uninfected controls. Interestingly, a 1.5- to 2-fold increase in the mRNA transcription of Cldn2 in the colon of EHEC-infected mice compared to uninfected control mice was demonstrated. The maximum increase in Cldn2 transcription occurred at 3 days post-infection but remained above baseline for up to 10 days. The increased Cldn2 transcription correlates with the increased claudin-2 expression in colonic samples as determined by immunofluorescence staining.

Discussion

EHEC can cause a wide spectrum of clinical outcomes ranging from non-bloody diarrhea to hemorrhagic colitis to life-threatening hemolytic-uremic syndrome. Stx is implicated in the development of hemorrhagic colitis and hemolytic-uremic syndrome. However, early symptoms of EHEC infection such as non-bloody diarrhea [22] are likely Stx-independent. Although previous *in vivo* models have been used to investigate the effects of EHEC infection [7, 12], most studies utilized germ-free or antibiotic-treated mice to optimize colonization of Stx-producing EHEC [13, 23, 24]. We were interested in examining the effects of EHEC organisms in the absence of Stx in a mouse model. We showed in this study that Stx-negative EHEC attach and colonize the intestinal tissue of C57Bl/6J mice resulting in structural and pathophysiological changes in the epithelium.

Previous mouse studies which utilized Stx-negative EHEC strains have suggested that the bacteria do not effectively colonize host intestines. Mundy et al compared the colonization potential of EHEC O157:H7 (strain Sakai), EPEC (strain E2348/69), *Citrobacter rodentium* (strain ICC169), and commensal *E. coli* (strain Nissle 1917) in C3H/Hej mice [25]. For the first 2 days post-infection, all strains were shed in stools at comparable numbers, but at day 3 post-infection fecal shedding of *C. rodentium* increased by 1.5-log and about 10^8 bacteria per gram stool was detected on days 3, 6, and 8. In contrast, no growth expansion phase of EHEC, EPEC and commensal *E. coli* was detected in the stool and only about 10^3–10^4 bacteria per gram stool were found at days 3, 6, and 8. Significantly lower levels of EHEC, EPEC and commensal *E. coli* were recovered from the intestinal tissues at day 8 post-infection, as compared to the levels of tissue-associated *C. rodentium*. They concluded that the EHEC and EPEC strains associated with the mouse intestine similar to the commensal *E. coli* strain.

For infected C57Bl/6J mice that did not receive antibiotics, the amounts of EHEC shed in the stool and associated with the different intestinal tissues at day 8 post-infection were comparable to those reported by Mundy and coworkers. However, in contrast with their results, we found growth expansions of EHEC in stools at day 8 post-infection and of tissue-associated EHEC at day 5 post-infection. In order for EHEC to colonize the host intestinal epithelium, the bacteria must first evade the host's innate immune system. The delayed growth of the colonizing EHEC in our model may be attributed to host's immune response, as well as to the adaptation of the bacteria to its new environment. For antibiotic-treated animals, growth expansion of colonizing EHEC was further delayed to day 8 post-infection. Since the EHEC strain we employed in this study is sensitive to streptomycin, the shift in bacterial growth expansion may be due to residual effects of the antibiotics.

Although EHEC colonize the intestine of C57Bl/6J mice that are not treated with antibiotics, improved bacterial colonization was attained by pre-treatment with streptomycin. Streptomycin disrupts the normal microflora of mouse intestines and enhances colonization of nonindigenous bacteria. Previously established mouse models utilizing streptomycin prior to and during infection have been shown to increase colonization of other pathogens such as *Salmonella typhimurium, Pseudomonas aeruginosa* and *Aeromonas* isolates [26–28]. Several mechanisms explaining enhanced colonization of nonindigenous bacteria in

streptomycin-treated animals include: (1) decreased competition between resident and nonindigenous bacteria for nutrients and attachment sites, and (2) environmental changes in the gut favoring colonization and growth of pathogens such increase in pH and decrease in short chain volatile fatty acids [27, 29, 30]. One limitation in the use of streptomycin in *in vivo* models of infection is that the pathogen being studied should be resistant to the antibiotics. In our study, the EHEC O157:H7 strain used was susceptible to streptomycin. In order to allow excretion of residual streptomycin, mice were allowed to recover for another 24 hours after antibiotic treatment before infecting with EHEC.

We demonstrated in this study that EHEC adhere to and colonize the cecum and colon more efficiently than the small intestine. While the mechanism of adherence was not assessed in this study, *in vitro* and some *in vivo* data suggests that fimbriae [31], outer membrane proteins [32], *iha*-encoded surface protein [33], and the TTSS [15] play a role in this process. Previous studies have shown that intimin contributes to the colonization of EHEC O157:H7 in mice. Female BALB/c mice immunized with a plant cell-based intimin vaccine prior to infection exhibited reduced duration of EHEC O157:H7 shedding in the stool [34]. In another study by O'Brien's group [35], infection of female BALB/c mice with intimin-deletion mutant of EHEC O157:H7 resulted to decreased colonization as compared to infection with the intimin-positive EHEC strain. In addition to the multiple factors involved in adherence, colonization in mouse models is also dependent on the mouse strain as demonstrated in a study by Nagano *et al* [15], wherein EHEC organisms were shown to effectively colonize ICR mice but not BALBc, C3H/HeN, C3H/HjN and A/J mice,

We also demonstrated that EHEC infection results in the distortion and effacement of microvilli. This correlates with actin rearrangement as observed in *in vitro* and *in vivo* studies [1, 15]. The effacement of microvilli and disruption of tight junctions by EHEC as demonstrated in C57Bl/6J mice has important clinical implications. Normally, intact microvilli structure and non-porous tight junctions help maintain the structural and physiological integrity of the gastrointestinal tract. Disruption of these homeostatic mechanisms of intestinal stability may contribute to the clinical effects of diarrhea as a consequence of EHEC infection.

Although EHEC induced localized effacement of microvilli, it was difficult to capture images of intimately attached bacteria and the well-characterized A/E lesions with pedestals due to modest levels of tissue-associated bacteria. Whole tissue imaging of infected bioluminescent EHEC, however, indicates that the bacteria associate tightly to the cecum and colon. At present, it is not clear if EHEC is able to induce microvilli effacement in the absence of intimately attached bacteria in the C57Bl/6J mice. Savkovic et al. [20] observed a similar phenotype in the enteropathogenic *E. coli* infection of C57Bl/6J mice. In contrast, previous studies on *C. rodentium* infection of mice [36, 37] and EHEC infection of rabbits and piglets [9, 38, 39] demonstrated intimately attached bacteria and A/E lesions with pedestals. The phenotypic differences between our model and those published for *C. rodentium* infection of mice and EHEC infection of rabbits and piglets may be due to differences in the bacteria, levels of colonizing bacteria and hosts used.

Once colonization and adherence to the intestines of C57Bl/6J mice occurs, EHEC infection results in physiological and structural changes of intestinal epithelial cells. Our study demonstrated alterations in these parameters by measuring TER and permeability to macromolecules and performing microscopic analysis of intestinal tissues. EHEC infection significantly reduced TER of the colon at 3 and 5 days post-infection in the absence of antibiotics and at days 8 and 10 post-infection in mice receiving streptomycin-pretreatment. We also verified that the decrease in TER detected in infected mice was accompanied by an increase in mucosal permeability to macromolecules. We further showed that the electrophysiological changes in the colon correlates with alterations in TJ architecture. Although ZO-1 was not altered as a result of EHEC infection, the redistribution of occludin and claudin-3 and increased expression of claudin-2 observed by immunohistochemistry correlate with the reduced TER observed in the colon.

Most interestingly, we showed, for the first time, that EHEC infection induces changes in claudin-2 expression in the crypts of mouse colon. Claudin-2 has been previously identified as the electrically ‘leaky’ claudin [40, 41] and its elevated expression has been implicated in inflammatory bowel disease [42, 43]. Expression of claudin-2 in CMT-93 and in MDCK cell lines was also shown to decrease TER [44, 45]. These previous studies corroborate our findings that elevated claudin-2 levels in the colon of EHEC-infected mice correlate with decreased TER.

We further showed that increased claudin-2 protein levels can be attributed to elevated amounts of mRNA transcripts. The half-life of claudin-2 protein expressed in MDCK cells is about 12 hours [46]. Hence, the increased claudin-2 protein levels we observed in our study are likely due to enhanced gene expression rather than protein accumulation.

Human CLDN2 and mouse Cldn2 gene promoters harbor binding sites for caudal-related homeobox (Cdx1 and Cdx2), hepatocyte-nuclear factor-1 alpha isoform (Hnf1α) and Gata4 transcription factors [47]. Mutagenesis and DNA-binding assays provided evidence that human CLDN2 promoter activity is positively regulated by Cdx2, as well as by Hnf1α[47, 48]. Forced expression of GATA4 in Caco-2 results in an increased claudin-2 expression [49]. In addition, the human CLDN2 gene promoter has an NFκB-binding site and deletion of this site decreased promoter activity in transfected Caco-2 cells [47]. NFκB is activated by TNFα, and high levels of TNFα are associated with the development of intestinal inflammation in Crohn’s disease. Interestingly, claudin-2 protein levels in human intestinal cell line HT-29 have been shown to increase in response to TNFα, and this was found to be due to elevated CLDN2-specific mRNA and enhanced promoter activity [50]. As EHEC also increases secretion of inflammatory cytokines, including TNFα, the increased Cldn2 gene expression we observed could either be a direct response to EHEC organisms or a secondary response to EHEC-induced TNFα secretion.

Claudin-3 is also upregulated in ulcerative colitis-associated colon carcinomas and in colorectal cancer [51, 52]. Increased expression of CLDN1, CLDN3 and CLDN4 in colorectal tumor tissues resulted in increased paracellular permeability and significant disorganization of tight junction strands observed via freeze fracture replicas [52]. CLDN3 knockdown by siRNA of human gastric adenocarcinoma cell line MKN28 decreased TER

[53]. In our study, low Cldn3 mRNA transcripts levels, combined with increased Cldn2 mRNA transcript levels, correlates with decreased TER at day 8 post-infection.

In addition to eletrophysiological changes and alterations in the distribution and expression of tight junction proteins, EHEC also induced mild inflammation as indicated by the increase in polymorphonuclear leukocytes at the lamina propria of colonic tissues at day 3 post-infection. It has been published previously that both EHEC and enteropathogenic *E. coli* attenuate the host immune response to infection [54–56]. Stx is also known to be pro-inflammatory [57, 58] but in our model system, we employed a Stx-negative strain. Hence, the lack of robust inflammatory phenotype in our study is not surprising.

In conclusion, our data demonstrates that C57Bl/6J mice are susceptible to infection by EHEC and serve as an appropriate *in vivo* model to establish the consequences of EHEC infection and define the role of specific EHEC effector molecules in pathogenesis.

Acknowledgments

Grant numbers and sources of support to Gail Hecht: NIH R01 DK058694, NIH P01 DK067887, VA Merit Award

This study was supported by grants R01 DK058694 and P01 DK067887 from the National Institute of Health to GH and by a Veterans Affairs Merit Award to GH. KJR is supported by the Crohn's & Colitis Foundation of America.

List of abbreviations

A/E	Attaching and Effacing
CFU	Colony Forming Units
EHEC	Enterohemorrhagic *Escherichia coli*
Stx	Shiga toxin
TEM	Transmission Electron Microscopy
TER	Transmucosal Electrical Resistance

References

1. Frankel G, Phillips AD, Rosenshine I, et al. Enteropathogenic and enterohaemorrhagic *Escherichia coli*: more subversive elements. Mol Microbiol. 1998; 30:911–921. [PubMed: 9988469]
2. McDaniel TK, Kaper JB. A cloned pathogenicity island from enteropathogenic *Escherichia coli* confers the attaching and effacing phenotype on *E. coli* K-12. Mol Microbiol. 1997; 23:399–407. [PubMed: 9044273]
3. Bielaszewska M, Karch H. Consequences of enterohaemorrhagic *Escherichia coli* infection for the vascular endothelium. Thromb Haemost. 2005; 94:312–318. [PubMed: 16113820]
4. Nataro JP, Kaper JB. Diarrheagenic *Escherichia coli*. Clin Microbiol Rev. 1998; 11:142–201. [PubMed: 9457432]
5. Viswanathan VK, Koutsouris A, Lukic S, et al. Comparative analysis of EspF from enteropathogenic and enterohemorrhagic *Escherichia coli* in alteration of epithelial barrier function. Infect Immun. 2004; 72:3218–3227. [PubMed: 15155623]
6. Hecht G, Marrero JA, Danilkovich A, et al. Pathogenic *Escherichia coli* increase Cl- secretion from intestinal epithelia by upregulating galanin-1 receptor expression. J Clin Invest. 1999; 104:253–262. [PubMed: 10430606]

7. Beery JT, Doyle MP, Schoeni JL. Colonization of chicken cecae by *Escherichia coli* associated with hemorrhagic colitis. Appl Environ Microbiol. 1985; 49:310–315. [PubMed: 3885853]
8. Potter ME, Kaufmann AF, Thomason BM, et al. Diarrhea due to Escherichia coli O157:H7 in the infant rabbit. J Infect Dis. 1985; 152:1341–1343. [PubMed: 3905989]
9. Pai CH, Kelly JK, Meyers GL. Experimental infection of infant rabbits with verotoxin-producing *Escherichia coli*. Infect Immun. 1986; 51:16–23. [PubMed: 3510166]
10. Francis DH, Moxley RA, Andraos CY. Edema disease-like brain lesions in gnotobiotic piglets infected with *Escherichia coli* serotype O157:H7. Infect Immun. 1989; 57:1339–1342. [PubMed: 2647636]
11. Tzipori S, Gunzer F, Donnenberg MS, et al. The role of the *eaeA* gene in diarrhea and neurological complications in a gnotobiotic piglet model of enterohemorrhagic *Escherichia coli* infection. Infect Immun. 1995; 63:3621–3627. [PubMed: 7642299]
12. Isogai E, Isogai H, Takeshi K, et al. Protective effect of Japanese green tea extract on gnotobiotic mice infected with an *Escherichia coli* O157:H7 strain. Microbiol Immunol. 1998; 42:125–128. [PubMed: 9572044]
13. Kurioka T, Yunou Y, Kita E. Enhancement of susceptibility to Shiga toxin-producing *Escherichia coli* O157:H7 by protein calorie malnutrition in mice. Infect Immun. 1998; 66:1726–1734. [PubMed: 9529103]
14. Ogawa M, Shimizu K, Nomoto K, et al. Protective effect of Lactobacillus casei strain Shirota on Shiga toxin-producing *Escherichia coli* O157:H7 infection in infant rabbits. Infect Immun. 2001; 69:1101–1108. [PubMed: 11160007]
15. Nagano K, Taguchi K, Hara T, et al. Adhesion and colonization of enterohemorrhagic *Escherichia coli* O157:H7 in cecum of mice. Microbiol Immunol. 2003; 47:125–132. [PubMed: 12680715]
16. Tzipori S, Karch H, Wachsmuth KI, et al. Role of a 60-megadalton plasmid and Shiga-like toxins in the pathogenesis of infection caused by enterohemorrhagic *Escherichia coli* O157:H7 in gnotobiotic piglets. Infect Immun. 1987; 55:3117–3125. [PubMed: 3316033]
17. Myhal ML, Laux DC, Cohen PS. Relative colonizing abilities of human fecal and K 12 strains of *Escherichia coli* in the large intestines of streptomycin-treated mice. Eur J Clin Microbiol. 1982; 1:186–192. [PubMed: 6756909]
18. Morin CE, Kaper JB. Use of stabilized luciferase-expressing plasmids to examine in vivo-induced promoters in the *Vibrio cholerae* vaccine strain CVD 103-HgR. FEMS Immunol Med Microbiol. 2009; 57:69–79. [PubMed: 19678844]
19. Wiles S, Pickard KM, Peng K, et al. In vivo bioluminescence imaging of the murine pathogen *Citrobacter rodentium*. Infect Immun. 2006; 74:5391–5396. [PubMed: 16926434]
20. Savkovic SD, Villanueva J, Turner JR, et al. Mouse model of enteropathogenic *Escherichia coli* infection. Infect Immun. 2005; 73:1161–1170. [PubMed: 15664959]
21. Shifflett DE, Clayburgh DR, Koutsouris A, et al. Enteropathogenic *E. coli* disrupts tight junction barrier function and structure in vivo. Lab Invest. 2005; 85:1308–1324. [PubMed: 16127426]
22. Mead PS, Griffin PM. *Escherichia coli* O157:H7. Lancet. 1998; 352:1207–1212. [PubMed: 9777854]
23. Shimizu K, Asahara T, Nomoto K, et al. Development of a lethal Shiga toxin-producing *Escherichia coli*-infection mouse model using multiple mitomycin C treatment. Microb Pathog. 2003; 35:1–9. [PubMed: 12860453]
24. Wadolkowski EA, Burris JA, O'Brien AD. Mouse model for colonization and disease caused by enterohemorrhagic *Escherichia coli* O157:H7. Infect Immun. 1990; 58:2438–2445. [PubMed: 2196227]
25. Mundy R, Girard F, FitzGerald AJ, et al. Comparison of colonization dynamics and pathology of mice infected with enteropathogenic *Escherichia coli*, enterohaemorrhagic *E. coli* and *Citrobacter rodentium*. FEMS Microbiol Lett. 2006; 265:126–132. [PubMed: 17034412]
26. Que JU, Hentges DJ. Effect of streptomycin administration on colonization resistance to *Salmonella typhimurium* in mice. Infect Immun. 1985; 48:169–174. [PubMed: 3884509]
27. Que JU, Casey SW, Hentges DJ. Factors responsible for increased susceptibility of mice to intestinal colonization after treatment with streptomycin. Infect Immun. 1986; 53:116–123. [PubMed: 3087876]

28. Lye DJ. A mouse model for characterization of gastrointestinal colonization rates among environmental *Aeromonas* isolates. Curr Microbiol. 2009; 58:454–458. [PubMed: 19130126]
29. Bohnhoff M, Miller CP, Martin WR. Resistance of the Mouse's Intestinal Tract to Experimental *Salmonella* Infection. I. Factors Which Interfere with the Initiation of Infection by Oral Inoculation. J Exp Med. 1964; 120:805–816. [PubMed: 14247721]
30. Bohnhoff M, Miller CP, Martin WR. Resistance of the Mouse's Intestinal Tract to Experimental Salmonella Infection. Ii. Factors Responsible for Its Loss Following Streptomycin Treatment. J Exp Med. 1964; 120:817–828. [PubMed: 14247722]
31. Karch H, Heesemann J, Laufs R, et al. A plasmid of enterohemorrhagic *Escherichia coli* O157:H7 is required for expression of a new fimbrial antigen and for adhesion to epithelial cells. Infect Immun. 1987; 55:455–461. [PubMed: 2879796]
32. Zhao S, Meng J, Doyle MP, et al. A low molecular weight outer-membrane protein of *Escherichia coli* O157:H7 associated with adherence to INT407 cells and chicken caeca. J Med Microbiol. 1996; 45:90–96. [PubMed: 8683557]
33. Tarr PI, Bilge SS, Vary JC Jr, et al. Iha: a novel *Escherichia coli* O157:H7 adherence-conferring molecule encoded on a recently acquired chromosomal island of conserved structure. Infect Immun. 2000; 68:1400–1407. [PubMed: 10678953]
34. Judge NA, Mason HS, O'Brien AD. Plant cell-based intimin vaccine given orally to mice primed with intimin reduces time of *Escherichia coli* O157:H7 shedding in feces. Infect Immun. 2004; 72:168–175. [PubMed: 14688094]
35. Sinclair JF, Dean-Nystrom EA, O'Brien AD. The established intimin receptor Tir and the putative eucaryotic intimin receptors nucleolin and beta1 integrin localize at or near the site of enterohemorrhagic *Escherichia coli* O157:H7 adherence to enterocytes in vivo. Infect Immun. 2006; 74:1255–1265. [PubMed: 16428775]
36. Mundy R, MacDonald TT, Dougan G, et al. *Citrobacter rodentium* of mice and man. Cell Microbiol. 2005; 7:1697–1706. [PubMed: 16309456]
37. Klapproth JM, Sasaki M, Sherman M, et al. *Citrobacter rodentium lifA/efa1* is essential for colonic colonization and crypt cell hyperplasia in vivo. Infect Immun. 2005; 73:1441–1451. [PubMed: 15731042]
38. Dean-Nystrom EA, Melton-Celsa AR, Pohlenz JF, et al. Comparative pathogenicity of *Escherichia coli* O157 and intimin-negative non-O157 Shiga toxin-producing *E coli* strains in neonatal pigs. Infect Immun. 2003; 71:6526–6533. [PubMed: 14573674]
39. Sherman P, Soni R, Karmali M. Attaching and effacing adherence of Vero cytotoxin-producing *Escherichia coli* to rabbit intestinal epithelium in vivo. Infect Immun. 1988; 56:756–761. [PubMed: 3278980]
40. Furuse M, Furuse K, Sasaki H, et al. Conversion of zonulae occludentes from tight to leaky strand type by introducing claudin-2 into Madin-Darby canine kidney I cells. J Cell Biol. 2001; 153:263–272. [PubMed: 11309408]
41. Amasheh S, Meiri N, Gitter AH, et al. Claudin-2 expression induces cation-selective channels in tight junctions of epithelial cells. J Cell Sci. 2002; 115:4969–4976. [PubMed: 12432083]
42. Weber CR, Nalle SC, Tretiakova M, et al. Claudin-1 and claudin-2 expression is elevated in inflammatory bowel disease and may contribute to early neoplastic transformation. Lab Invest. 2008; 88:1110–1120. [PubMed: 18711353]
43. Zeissig S, Burgel N, Gunzel D, et al. Changes in expression and distribution of claudin 2, 5 and 8 lead to discontinuous tight junctions and barrier dysfunction in active Crohn's disease. Gut. 2007; 56:61–72. [PubMed: 16822808]
44. Van Itallie CM, Holmes J, Bridges A, et al. The density of small tight junction pores varies among cell types and is increased by expression of claudin-2. J Cell Sci. 2008; 121:298–305. [PubMed: 18198187]
45. Inai T, Sengoku A, Hirose E, et al. Comparative characterization of mouse rectum CMT93-I and -II cells by expression of claudin isoforms and tight junction morphology and function. Histochem Cell Biol. 2008; 129:223–232. [PubMed: 18034259]

46. Van Itallie CM, Colegio OR, Anderson JM. The cytoplasmic tails of claudins can influence tight junction barrier properties through effects on protein stability. J Membr Biol. 2004; 199:29–38. [PubMed: 15366421]
47. Sakaguchi T, Gu X, Golden HM, et al. Cloning of the human claudin-2 5′-flanking region revealed a TATA-less promoter with conserved binding sites in mouse and human for caudal-related homeodomain proteins and hepatocyte nuclear factor-1alpha. J Biol Chem. 2002; 277:21361–21370. [PubMed: 11934881]
48. Mankertz J, Hillenbrand B, Tavalali S, et al. Functional crosstalk between Wnt signaling and Cdx-related transcriptional activation in the regulation of the claudin-2 promoter activity. Biochem Biophys Res Commun. 2004; 314:1001–1007. [PubMed: 14751232]
49. Escaffit F, Boudreau F, Beaulieu JF. Differential expression of claudin-2 along the human intestine: Implication of GATA-4 in the maintenance of claudin-2 in differentiating cells. J Cell Physiol. 2005; 203:15–26. [PubMed: 15389642]
50. Mankertz J, Amasheh M, Krug SM, et al. TNFalpha up-regulates claudin-2 expression in epithelial HT-29/B6 cells via phosphatidylinositol-3-kinase signaling. Cell Tissue Res. 2009
51. de Oliveira SS, de Oliveira IM, De Souza W, et al. Claudins upregulation in human colorectal cancer. FEBS Lett. 2005; 579:6179–6185. [PubMed: 16253248]
52. Mees ST, Mennigen R, Spieker T, et al. Expression of tight and adherens junction proteins in ulcerative colitis associated colorectal carcinoma: upregulation of claudin-1, claudin-3, claudin-4, and beta-catenin. Int J Colorectal Dis. 2009; 24:361–368. [PubMed: 19184060]
53. Hashimoto K, Oshima T, Tomita T, et al. Oxidative stress induces gastric epithelial permeability through claudin-3. Biochem Biophys Res Commun. 2008; 376:154–157. [PubMed: 18774778]
54. Hauf N, Chakraborty T. Suppression of NF-kappa B activation and proinflammatory cytokine expression by Shiga toxin-producing *Escherichia coli*. J Immunol. 2003; 170:2074–2082. [PubMed: 12574378]
55. Sharma R, Tesfay S, Tomson FL, et al. Balance of bacterial pro- and anti-inflammatory mediators dictates net effect of enteropathogenic *Escherichia coli* on intestinal epithelial cells. Am J Physiol Gastrointest Liver Physiol. 2006; 290:G685–694. [PubMed: 16322091]
56. Bellmeyer A, Cotton C, Kanteti R, et al. Enterohemorrhagic *Escherichia coli* suppresses inflammatory response to cytokines and its own toxin. Am J Physiol Gastrointest Liver Physiol. 2009; 297:G576–581. [PubMed: 19556613]
57. Ritchie JM, Thorpe CM, Rogers AB, et al. Critical roles for *stx2*, *eae*, and *tir* in enterohemorrhagic *Escherichia coli*-induced diarrhea and intestinal inflammation in infant rabbits. Infect Immun. 2003; 71:7129–7139. [PubMed: 14638803]
58. Yamasaki C, Natori Y, Zeng XT, et al. Induction of cytokines in a human colon epithelial cell line by Shiga toxin 1 (Stx1) and Stx2 but not by non-toxic mutant Stx1 which lacks N-glycosidase activity. FEBS Lett. 1999; 442:231–234. [PubMed: 9929007]

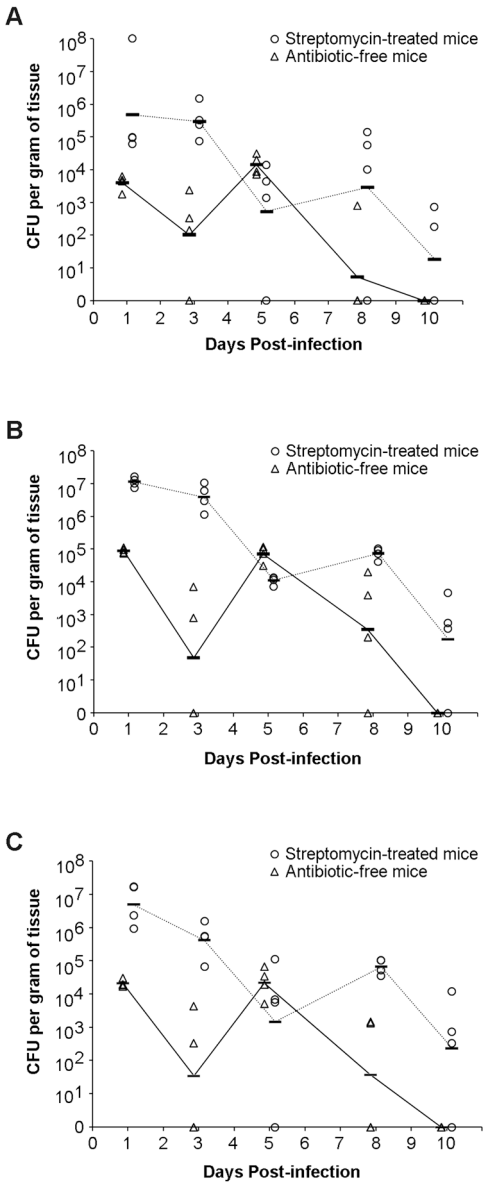

Figure 1.

Localization of *E. coli* O157:H7 in mouse intestines. The presence of *E. coli* O157:H7 in the ileum (A), cecum (B), and proximal colon (C) of infected C57Bl/6J mice was determined at 1, 3, 5, 8 and 10 days post-infection. Group geometric mean of CFU per gram of tissue is shown for infected mice that did not receive antibiotics (triangles) and for mice treated with streptomycin prior to EHEC infection (circles).

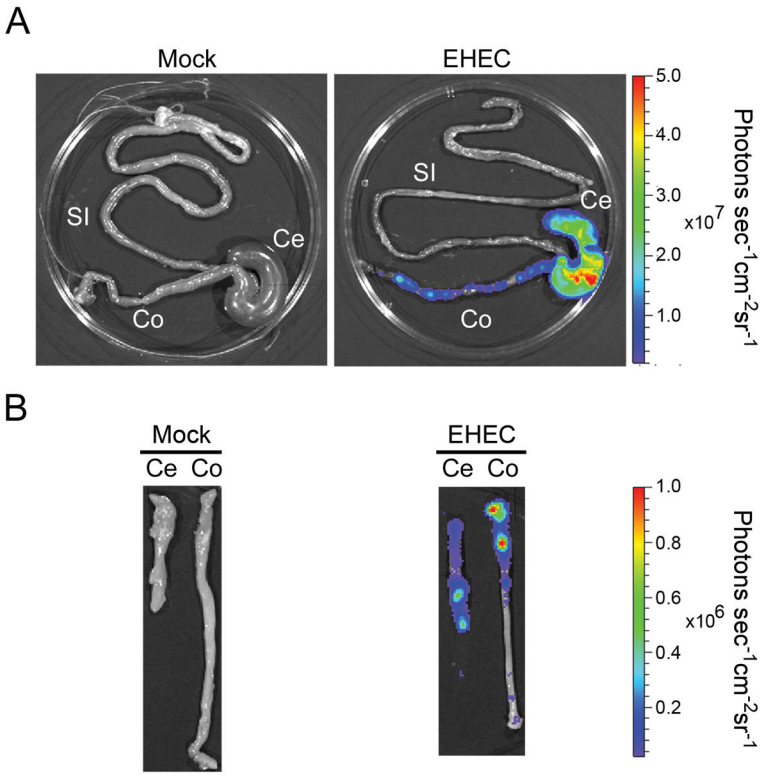

Figure 2.

Imaging of intestinal tissues of streptomycin-pretreated mice infected with bioluminescent EHEC. (A) The entire intestine (si, small intestine; ce, cecum; co, colon) was excised from mice orally infected with bioluminescent EHEC for three days. A pseudocolor image depicting bioluminescence intensity (*red*, more intense; *blue*, less intense) was generated using Living Image® Software (Xenogen) and superimposed onto the photographic image. The color bar indicates relative signal intensity (photons s^{-1} cm^{-2} sr^{-1}). (B) Thereafter, the cecum and colon were opened longitudinally and washed with PBS prior to imaging with IVIS. Data representative of EHEC- infected (n=9) and Mock-infected (n=5) mice from two separate experiments.

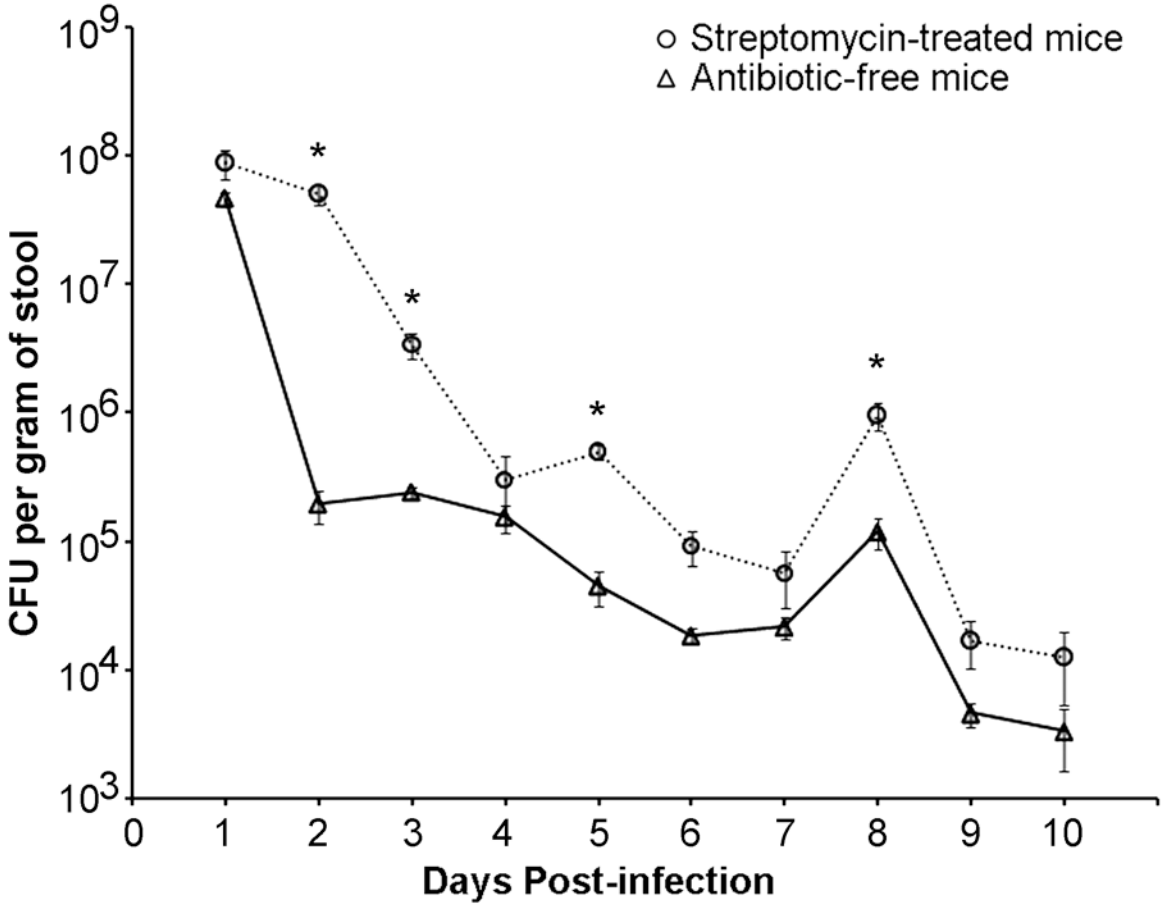

Figure 3.

Fecal shedding of *E. coli* O157:H7 in mice following inoculation with the pathogen. C57Bl/6J mice were orally gavaged with 2×10^8 of *E. coli* O157:H7 and their feces were monitored for the presence of bacteria over a period of 10 days. Group geometric mean of CFU per gram of feces is shown for infected mice that did not receive antibiotics (triangles) and for mice treated with streptomycin prior to EHEC infection (circles). * indicates $p_{value} < 0.05$ when daily fecal shedding of EHEC in antibiotic-free mice and streptomycin-pretreated mice are compared.

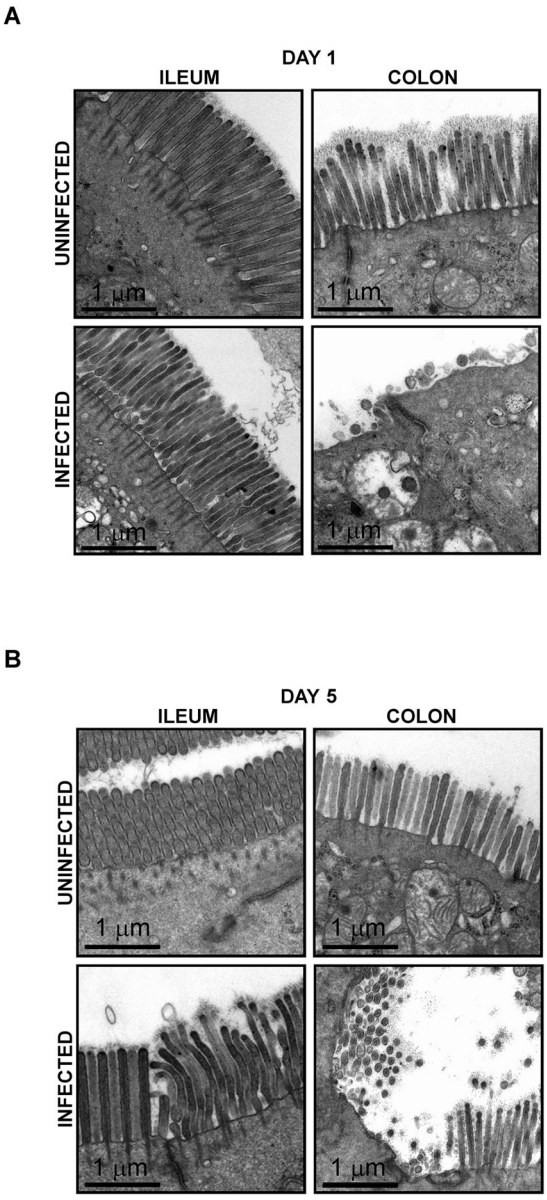

Figure 4.

Electron micrograph images of the ileum and colon of uninfected and EHEC-infected antibiotic-free C57Bl/6J mice at day 1 (A) and day 5 (B) post-infection. Scale bar = 1 μm.

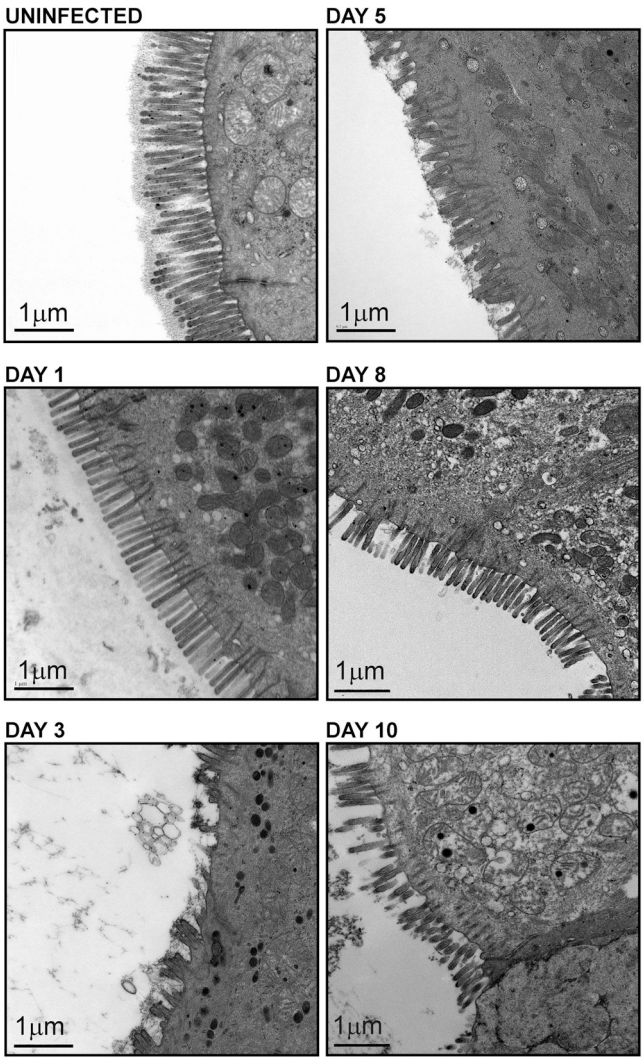

Figure 5.
Electron micrograph images of colonic tissues from uninfected and EHEC-infected C57Bl/6J mice pre-treated with streptomycin at days 1, 3, 5, 8 and 10 post-infection. Scale bar = 1 μm.

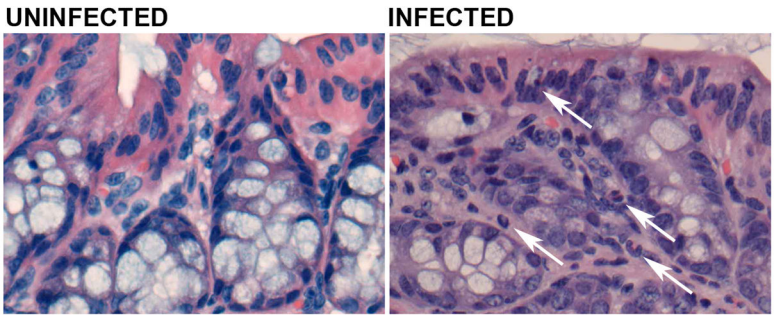

Figure 6.

Hematoxylin and eosin staining of colonic tissues from uninfected and EHEC-infected C57Bl/6J mice pre-treated with streptomycin at day 3 post-infection. Arrows point to lamina propria polymorphonuclear leukocytes.

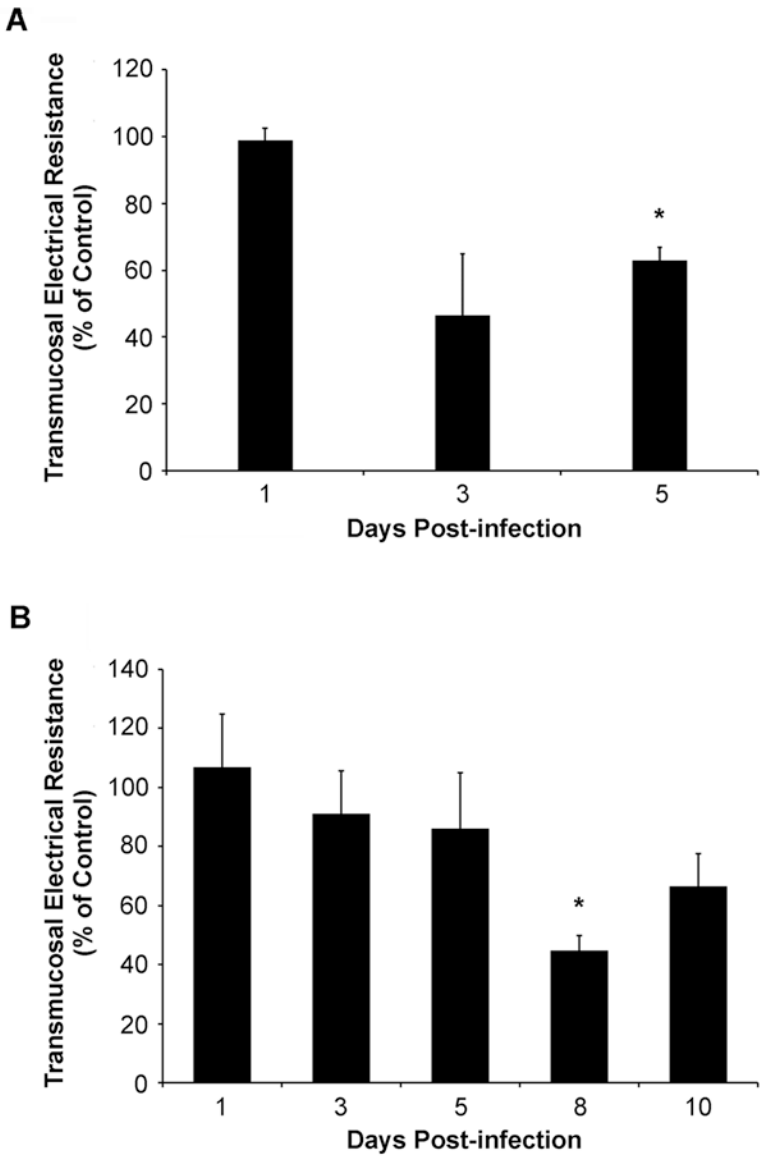

Figure 7.

Transmucosal electrical resistance (TER) of colonic tissues from antibiotic-free C57Bl/6J mice infected with EHEC (A) and mice pre-treated with streptomycin (B). Segments of colonic tissues were mounted in Üssing chambers and TER values were determined. Group geometric means of TER of colons of infected mice are shown as percent of uninfected control mice. * indicates $p_{value} < 0.05$ when daily TER values of colonic tissues from infected mice are compared to uninfected control mice.

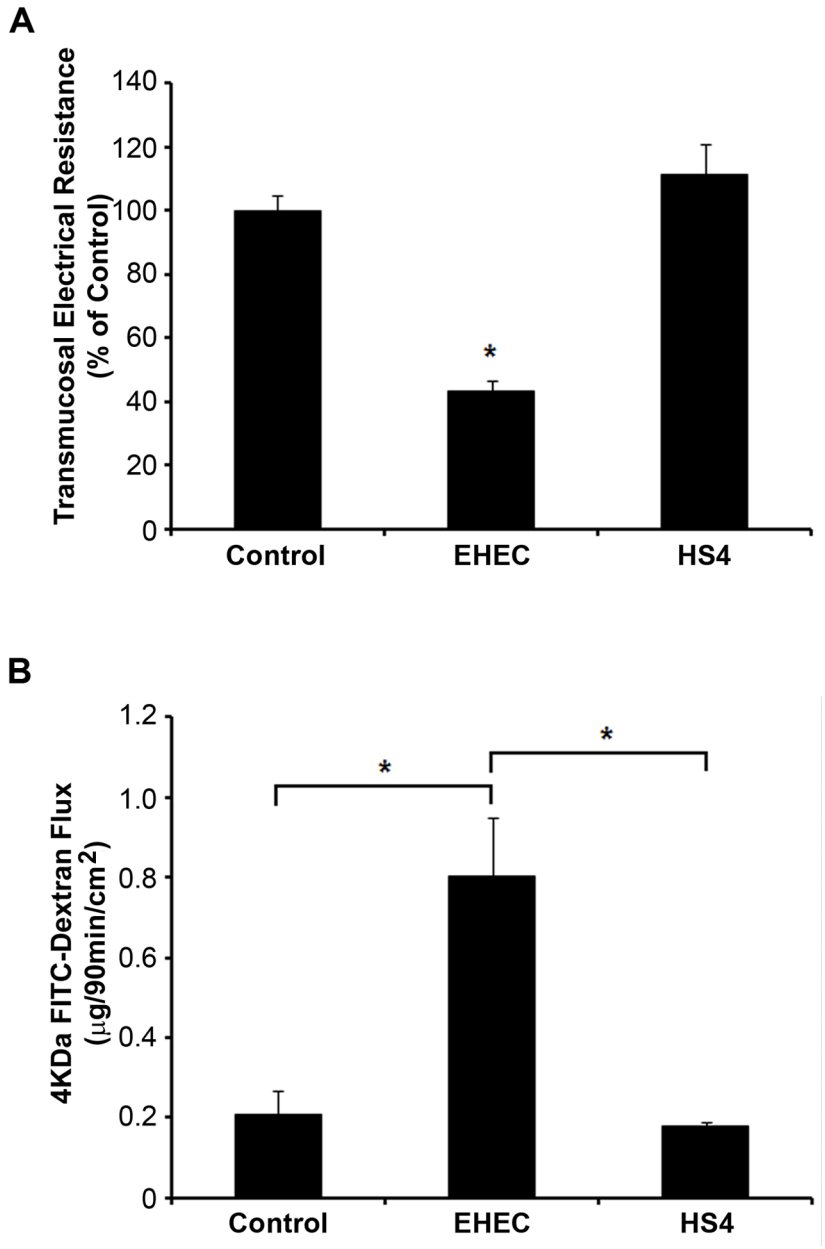

Figure 8.

Mucosal permeability to 4-KDa FITC-dextran of colonic tissues from infected mice pre-treated with streptomycin at day 8 post-infection. (A) Transmucosal electrical resistance of colonic tissues from uninfected, EHEC- and HS-4-infected mice. (B) Flux of 4-KDa FITC-dextran across mouse colonic tissues from uninfected, EHEC- and HS-4 infected mice determined at the end of a 90-minute experimental period. * indicates indicates $p_{value} < 0.01$.

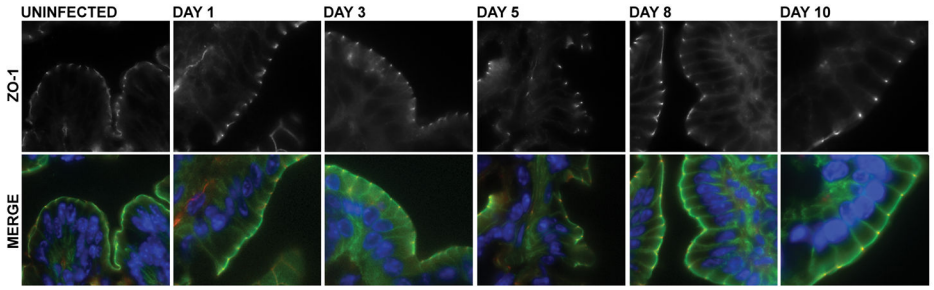

Figure 9.

ZO-1 immunofluorescence microscopy of colonic tissues from uninfected and EHEC-infected C57Bl/6J mice pre-treated with streptomycin at days 1, 3, 5, 8 and 10 post-infection. Merged image shows ZO-1 (red), actin (green) and Hoechst (blue) staining of colonic samples.

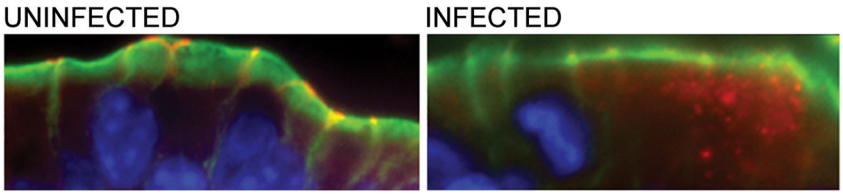

Figure 10.

Occludin immunofluorescence microscopy of colonic tissues of uninfected and EHEC-infected C57Bl/6J mice pre-treated with streptomycin at day 5 post-infection. Colonic tissues were stained for occludin (red), actin (green) and Hoechst (blue).

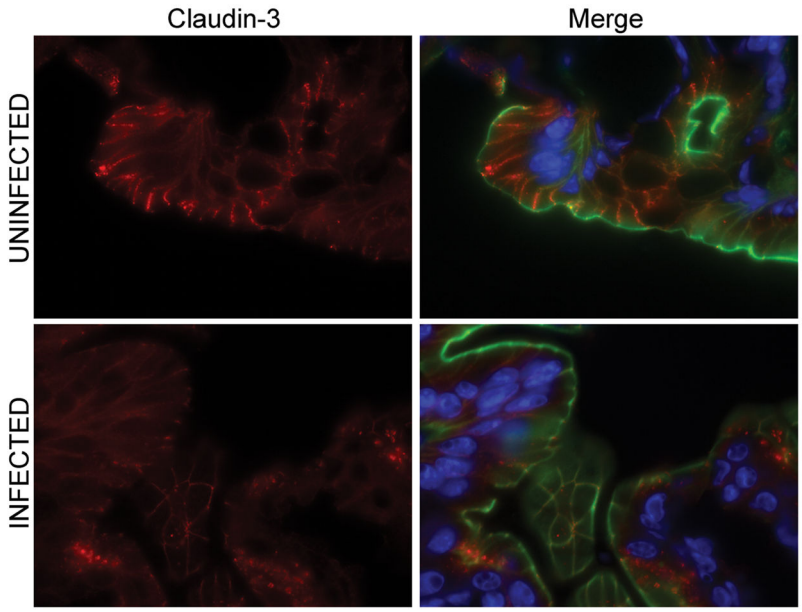

Figure 11.

Claudin-3 immunofluorescence microscopy of colonic tissues of uninfected and EHEC-infected C57Bl/6J mice pre-treated with streptomycin at day 3 post-infection. Merged image shows claudin-3 (red), actin (green) and Hoechst (blue) staining of colonic samples.

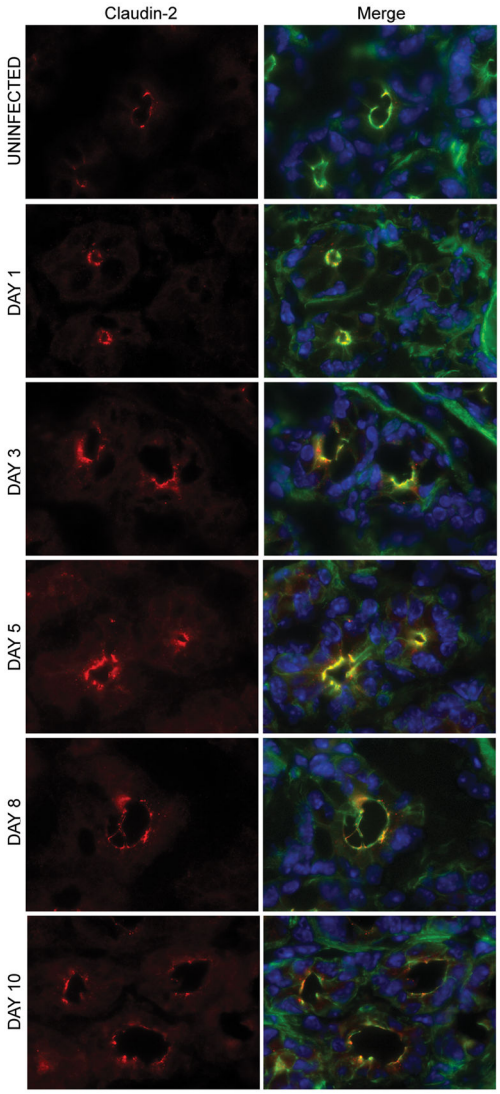

Figure 12.

Claudin-2 immunofluorescence microscopy of colonic tissues from uninfected and EHEC-infected C57Bl/6J mice pre-treated with streptomycin at days 1, 3, 5, 8 and 10 post-infection. Merged image shows claudin-2 (red), actin (green) and Hoechst (blue) staining of colonic samples.

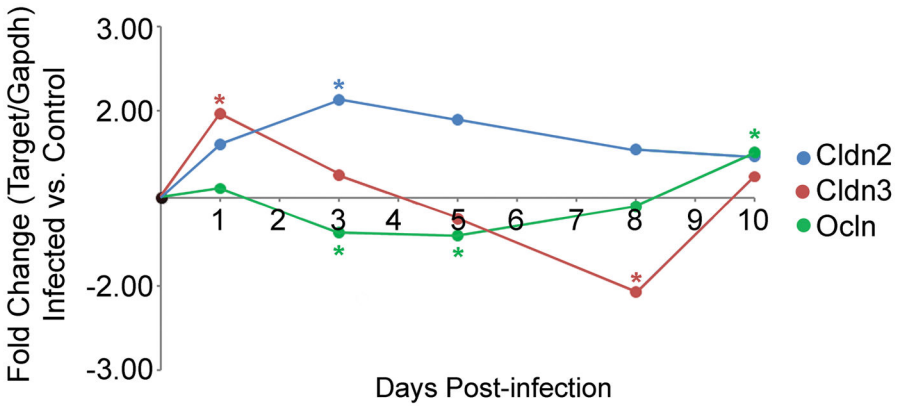

Figure 13.

mRNA transcript levels of Cldn2, Cldn3 and Ocln present in colonic tissues of uninfected and EHEC-infected C57Bl/6J mice pre-treated with streptomycin at days 1, 3, 5, 8 and 10 post-infection. Fold change of target mRNA copies per *gapdh* mRNA copies of colon samples of EHEC-infected mice compared to uninfected controls were determined. Values above x-axis are positive fold changes, and values below x-axis are negative fold changes. * indicates $p_{value} < 0.05$ when daily target mRNA transcript levels present in colonic tissues of infected mice are compared to uninfected control mice.